AGU PUBLICATIONS

Water Resources Research

RESEARCH ARTICLE
10.1002/2014WR016539

Chute cutoff as a morphological response to stream reconstruction: The possible role of backwater

J. P. C. Eekhout[1] and A. J. F. Hoitink[1]

[1]Hydrology and Quantitative Water Management Group, Wageningen University, Wageningen, Netherlands

Key Points:
- Detailed process analysis of a chute cutoff event in a reconstructed stream
- Chute cutoff explained from a backwater effect that forms a plug bar
- Despite the artificial setting there are similarities with natural rivers

Correspondence to:
A. J. F. Hoitink,
Ton.Hoitink@wur.nl

Citation:
Eekhout, J. P. C., and A. J. F. Hoitink (2015), Chute cutoff as a morphological response to stream reconstruction: The possible role of backwater, *Water Resour. Res.*, *51*, 3339–3352, doi:10.1002/2014WR016539.

Received 10 OCT 2014
Accepted 7 APR 2015
Accepted article online 14 APR 2015
Published online 8 MAY 2015

Abstract Stream restoration efforts often aim at creating new unconstrained meandering channels without weirs and bank revetments. In reconstructed streams, the initial morphological response of the new streams is often rapid, until a dynamic equilibrium is reached. Here we report on a chute cutoff that occurred within 3 months after realization of a stream restoration project, caused by a plug bar that formed in response to a backwater effect. The temporal evolution of the morphology of both the new and the old channels was monitored over a period of nearly 8 months, including precutoff conditions. The observations can be separated into three stages. Stage 1 is the initial period leading to cutoff vulnerability, stage 2 is the actual cutoff, and stage 3 is the morphological adjustment in response to the cutoff. In stage 1, a plug bar was deposited in one of the channel bends. Hydrodynamic model results show the location of the plug bar coincides with a region where bed shear stress decreased in downstream direction due to backwater. Longitudinal channel bed profiles show that the channel slope decreased soon after channel reconstruction. Hence, sediment from upstream was available to form the plug bar. After the plug bar was deposited, an embayment formed in the floodplain at a location where the former channel was located (stage 2). The former channel was filled with sediment prior to channel construction. It is likely that the sediment at this location was less consolidated, and therefore, prone to erosion. The chute channel continued to incise and widen into the floodplain and, after 6 months, acted as the main channel, conveying the discharge during the majority of time (stage 3). The cutoff channel gradually continued to fill with sediment, from the moment the plug bar formed until the chute channel incised into the floodplain. Sedimentary successions of the deposited material show upward fining, which is in agreement with observations of chute cutoffs in rivers. Although the artificial setting limits the degree in which the observed processes can be projected on natural rivers, the observations prompt to investigate the role of backwater effects in natural chute cutoff initiation.

1. Introduction

To counter the global decline in biodiversity and improve hydrological functioning of catchments, streams are being restored with an increasingly objective-based strategy [*Dufour and Piégay*, 2009]. In lowland countries like the Netherlands, restoration programs generally involve the removal of bank revetments and weirs, to create new unconstrained channels with vegetated banks. Streams in agricultural areas are being reconstructed to become more sinuous. This improves the landscape values and buffers the discharge by increasing the length of the stream. The initial morphological response of newly created streams is often rapid, which can be interpreted as a development toward a new dynamic morphological equilibrium. *Eekhout et al.* [2014a] described a morphological regime change that occurred within the first 2 years after reconstruction of a stream called Lunterse Beek, which was attributed to the growth of vegetation and variation in sediment supply. Here we analyze the detailed processes that have led to the formation of a chute cutoff that occurred within the first 3 months after reconstruction finished in the Lunterse Beek, and explore the possible links with chute cutoffs in natural rivers.

A chute cutoff can be defined as the formation of a new channel across an inner bend sediment deposit or floodplain peninsula enclosed by a meander loop, which typically results in gradual closure of the abandoned channel by sedimentation. The new channel is referred to as the chute channel, and the abandoned channel as the cutoff channel. A chute cutoff differs from a neck cutoff, which can be defined as the self-intersection of an evolving meander bend. Three mechanisms have been proposed in the literature to

explain chute cutoff vulnerability: (1) swale enlargement, (2) headcut propagation, and (3) embayment formation and extension [*Constantine et al*., 2010]. According to the first mechanism, a local depression in the floodplain may channelize the flow during a flood, carving a channel aligned with a former course of the river [*Hickin and Nanson*, 1975]. The second mechanism refers to a headcut at the downstream boundary of a meander bend, caused by a concentrated floodplain flow plunging over a river bank, back into the channel. The floodplain flow, in turn, may result from a debris dam in the river, steering the flow up against a river bank. This chute cutoff mechanism mainly occurs in rivers with floodplains consisting of cohesive sediment, which acts to maintain the form of the headcut [*Brush and Wolman*, 1960; *Gay et al*., 1998]. The third mechanism considers the formation of an embayment as a result of localized bank erosion where flow impinges on an outer bank, upstream of the meander that undergoes cutoff. Subsequent floods extend the embayment, shifting it downstream until it intersects the riverbank downstream, forming a chute channel [*Constantine et al*., 2010]. The classification above applies to natural rivers, which may or may not be applicable to reconstructed streams. Here we demonstrate that a chute cutoff in the Lunterse Beek was preceded by the formation of an embayment, where sediment deposition in the main channel obstructed the flow.

Regarding field-based observations taken when a cutoff channel forms, there are only a few case studies available. Most of these offer qualitative rather than quantitative information, giving insight into the causal relationships involved in processes during chute cutoff events. The majority of these studies claim that the chute cutoffs under study occurred during periods of overbank flow [*Johnson and Paynter*, 1967; *Hooke*, 1995; *Gay et al*., 1998; *Zinger et al*., 2011]. This was also observed under laboratory conditions [*Jin and Schumm*, 1987; *Peakall et al*., 2007; *Braudrick et al*., 2009; *Van Dijk et al*., 2012]. Even though these experiments were performed imposing discharges at the upstream boundary that were aimed at bankfull conditions, overbank flow did occur, caused by changes in channel slope [*Jin and Schumm*, 1987] and in-channel sedimentation [*Van Dijk et al*., 2012]. Both field and lab studies show overbank flow is an inherent feature of the occurrence of chute cutoffs, although the magnitude and return frequency of the floods needed for chute channels to develop is still unknown and may vary.

Existing quantitative field studies have focused on processes of sedimentation in cutoff channels and on postcutoff morphodynamics in chute channels. Sedimentation processes in cutoff channels were investigated shortly after the cutoff occurred [*Johnson and Paynter*, 1967; *Thompson*, 1984; *Hooke*, 1995; *Dieras et al*., 2013] and at sites where historical evidence was present [*McGowen and Garner*, 1970; *Erskine et al*., 1992; *Constantine et al*., 2010; *Ghinassi*, 2011]. Sedimentation of the cutoff channel exhibits a fining-upward sequence, from coarse sand, gravel, or cobbles at the base to clay loam or sand at the surface [e.g., *Erskine et al*., 1992; *Hooke*, 1995]. Differences in grain size characteristics of the deposited material are related to the flow regime after the channel underwent cutoff. In a laboratory experiment, *Peakall et al*. [2007] showed that deposition of fine to medium sands (corresponding to the coarser material in the experiment) coincides with continued flow through the cutoff, whereas deposition of fine-grained fills of clays and loams coincides with slow-moving or stagnant water in the cutoff channel.

Only recently, case studies describing postcutoff morphodynamics were presented in the literature, where the collection of the morphological data mainly focused on the chute channel. *Fuller et al*. [2003] quantified in detail the magnitudes of sediment transfers associated with channel adjustments following cutoff, in a laterally active gravel-bed river. Their analysis shows that the initial morphological development was dominated by bed scour, followed by a period of extensive bank erosion and lateral channel migration. *Zinger et al*. [2011] estimated the amount of sediment produced by two chute cutoff events. They found that each event triggered the rapid delivery of sediment into the river, at rates 1–5 orders of magnitude larger than those produced by lateral migration of individual bends. They also found that much of this material was deposited immediately downstream, which led to significant changes in channel morphology. The authors performed measurements of flow velocity and morphology, leading to a conceptual model of chute-cutoff dynamics in which the upstream and downstream ends of a cutoff channel are treated as a bifurcation and confluence, respectively [*Zinger et al*., 2013].

The lack of process-based field studies is the main reason why the physical controls on processes of chute cutoff formation remain poorly understood [*Grenfell et al*., 2012]. This hampers the use of knowledge from natural rivers in the context of stream restoration. Despite this, there have been several attempts to model the process of chute cutoff. Chute cutoff initiation has been incorporated into a one-dimensional meander migration model by *Howard* [1996]. The model does not capture the flood flow across the point bar creating

the chute cutoff, but predicts the influence of planform and topographic characteristics determining where and when chute cutoffs are expected to occur. *Constantine et al*. [2010] applied a two-dimensional depth-averaged hydrodynamic model to determine the influence of the channel curvature on the location where overbank flow incises the floodplain, causing the initial chute cutoff formation. *Constantine et al*. [2010] suggest that chute cutoff initiation is due to overbank flow escaping from the main channel, where the riverbank most strongly turns away from the downstream flow path. Recently, *Van Dijk et al*. [2014] applied 1-D and 3-D models to study several hydrological and morphological scenarios related to chute cutoffs. They found that chute cutoffs are more likely to occur under the combined conditions of overbank flow and a gradient advantage between the cutoff channel and the chute channel. The curvature at the bifurcation between the cutoff and chute channel determined the success rate of the chute cutoff.

Unlike other morphological processes that occur in meandering channels (e.g., bank erosion, neck cutoffs, meander migration), detailed analysis of field observations of chute cutoffs are still lacking [*Micheli and Larsen*, 2011]. Observations are needed to better understand the mechanisms that can lead to a chute cutoff, and to obtain data sets allowing to establish and improve the predictive capacity of numerical models needed in the context of stream restoration [e.g., *Langendoen*, 2011]. Based on a data set that has been made publicly available, here we present field evidence revealing that backwater effects may play a crucial role in creating a decelerating flow that leads to plug bar formation and an impinging flow causing a chute cutoff event.

2. Study Area

In October 2011, a stream restoration project was realized in a small lowland stream (Lunterse Beek) located in the central part of the Netherlands (52°4′46″N, 5°32′30″E), see Figure 1. The goal of the restoration plan was to improve ecological conditions, increasing the flora and fauna inside the stream and across the adjacent floodplain within the boundaries of hydrological constraints, such as maintaining groundwater levels for adjacent agricultural fields and preventing floods. *Eekhout et al*. [2014b] offer a general introduction to stream restoration in the Netherlands, and evaluate the morphological developments in the Lunterse Beek and two other streams, including habitat pattern development. They argue that the current design procedures are deficient to reach the flow velocity and water depth targets. This motivates the present local study focusing on a chute cutoff, which contributes to better understanding of morphological processes. This may eventually help to improve design procedures. More elaborate descriptions of the local context and the complete data set where this paper is based on can be found in *Eekhout et al*. [2014a, 2014b].

Over a total length of 1.6 km, a sinuous planform (with a sinuosity of 1.24) replaced a former straightened channel, where the course of the new channel crossed the former channel at several locations (Figure 1c). The channel was constructed with a channel width of 6.5 m, a channel depth of 0.4 m, and a channel slope of 0.96 m km^{-1}. The floodplain surrounding the channel was lowered as part of the restoration project, and has an average width of 20 m (Figures 1e and 4a). At the downstream end of the study area, a bridge reduces the floodplain width to less than 10 m (Figure 1e). The bed material mainly consists of medium to fine sand, with a median grain size of 258 μm. In a 20 m channel reach, located upstream from the main study area, the bed and banks consist of peat (Figure 1d).

Figure 1b shows the location of the study area in the catchment. The catchment has an area of 63.6 km^2. The elevation within the catchment varies from 3 to 25 m above mean sea level. The study area is located in a mildly sloping area. Figure 1e shows two cross sections in the study area, illustrating the lowered floodplain and the width reduction at the bridge location. The reconstructed channel has a composite profile, with a main channel that exceeds bankfull conditions about 30% of time, within 1 year. The subsurface of the catchment mainly consists of aeolian-sand deposits. Agriculture is the main land-use in the catchment [*Eekhout et al*., in press]. The average yearly precipitation amounts to 793 mm [*KNMI*, 2014]. The average daily discharge is measured at 0.33 $m^3\ s^{-1}$ and the peak discharge during the study period was 5.67 $m^3\ s^{-1}$.

3. Materials and Methods

3.1. Morphological Monitoring

The temporal evolution of the bathymetry has been monitored over a period of almost 2 years. Here we concentrate on the initial 8 months, including five GPS surveys and one ADCP survey. Morphological data

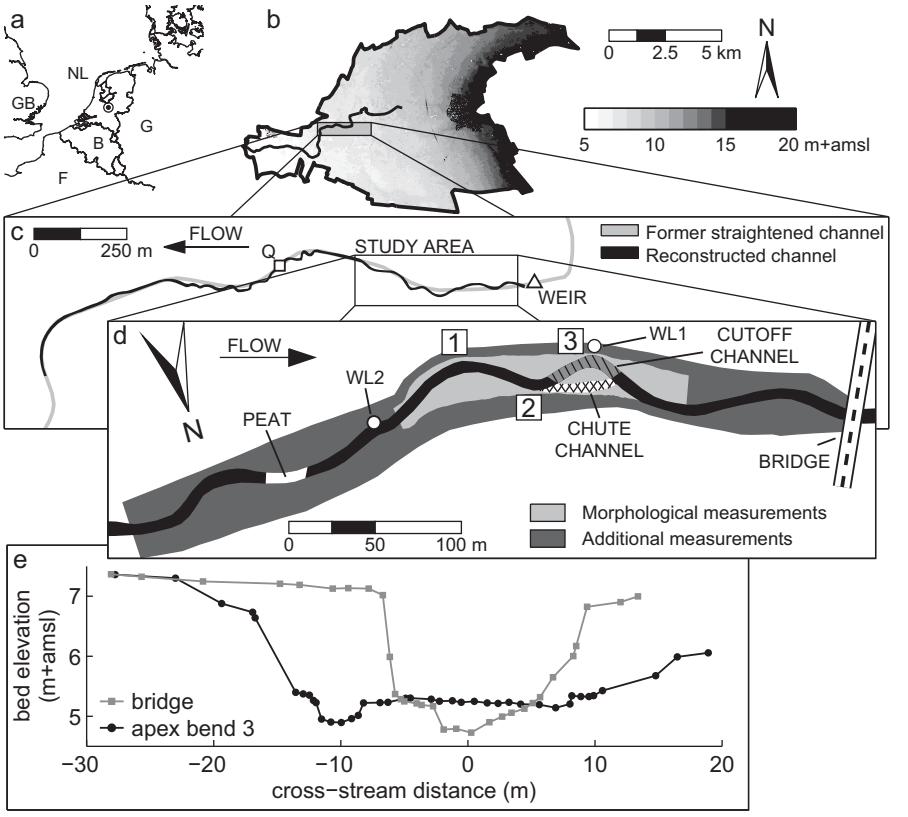

Figure 1. Overview of the study area: (a) location of the study area in the Netherlands, (b) elevation model of the catchment, (c) planform of the reconstructed channel, with the squared marker indicating the location of the discharge station (Q) and the triangular marker the location of a weir (WEIR), and (d) sketch of the study area, indicating the location of the cutoff and chute channels, the location of the peat deposit, the location of a bridge at the downstream end of the study area, the location of the water level gauges with circled markers and the three main bends with labels 1–3, and (e) bed elevation along two cross sections in the study area, illustrating the lowered floodplain (apex of bend 3) and the narrow section at the bridge location.

were collected in the area within the lowered floodplain over a length of 180 m, indicated by light gray in Figure 1d. Morphological data were collected with an average frequency of 46 days, using Real Time Kinematic (RTK) GPS equipment (Leica GPS 1200+) to measure channel bed surface elevation with an accuracy between 1 and 2 cm. The surface elevation data were collected along cross sections between the two floodplain edges. The survey strategy proposed by *Milan et al*. [2011] was followed, focusing on breaks of slope. Following this strategy, the point density was increased in the vicinity of steep slopes (e.g., channel banks), and decreased at flat surfaces (e.g., floodplains). Digital Elevation Models (DEMs) and DEMs of Difference (DoDs) of each of the 14 data sets were constructed, see *Eekhout et al*. [2014a]. Table 1 lists the point density and anisotropy factors for the six surveys used here, specified for the channel and floodplain sections.

Table 1. Overview of the Six Morphological Measurements, Showing the Survey Date, the Surveying Equipment, the Number of Data Points, the Point Density (PD) in Points m^{-2} and the Anisotropy Factor (AF) as Used in the Interpolation Routine, Specified for the Channel and Floodplain Data

Measurement No.	1	2	3	4	5	6
Survey date	12 Oct 2011	15 Dec 2011	13 Jan 2012	22 Feb 2012	20 Apr 2012	30 May 2012
Survey date (day)	0	64	93	133	191	231
Equipment	RTK-GPS	ADCP	RTK-GPS	RTK-GPS	RTK-GPS	RTK-GPS
No. data points	379	8394	956	918	742	1158
PD (all)	0.16	2.46	0.32	0.27	0.20	0.30
PD (channel)	0.25	4.09	0.44	0.34	0.31	0.45
AF (channel)	10.51	11.70	5.30	3.74	4.42	4.19
PD (floodplain)	0.12	2.21	0.24	0.24	0.15	0.24
AF (floodplain)	4.95	12.15	2.47	2.25	2.13	2.09

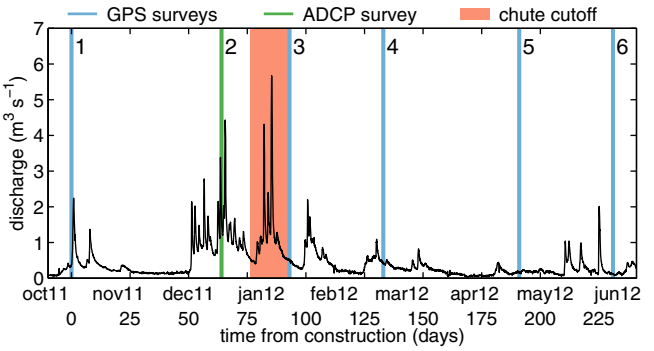

Figure 2. Discharge hydrograph for the channel under study. The morphological surveys are indicated with the blue and green vertical lines for the GPS and ADCP surveys, respectively. The chute cutoff took place in the period indicated in red.

Measurements taken with an acoustic Doppler current profiler (ADCP) offered additional information on bed level information, since the acoustic beams track the bottom. Despite accuracy limitations, the bed level data from the ADCP survey appeared valuable to the present study, as the survey took place just before the cutoff event. The ADCP survey was undertaken with a Teledyne RDI StreamPro ADCP. The StreamPro ADCP was mounted on a float, with a length of 0.70 m and a width of 0.43 m. The ADCP used four acoustic beams to measure the depth of the channel relative to the ADCP transducer, with a sampling frequency of 0.5 Hz. Bed level data were recorded for water depths exceeding 0.10 m. The track of the float was measured using bottom tracking. An RTK-GPS antenna (Septentrio Altus APS-3) was mounted on the ADCP to be able to transform the local coordinates and measured channel depths to the Dutch coordinate system (RD-coordinates) and to elevation above mean sea level.

From four morphological surveys (three GPS surveys and the ADCP survey), bed elevation data were also obtained in the channel upstream from the study area. These measurements were focused on the channel bed rather than on the floodplain. Both data sets were combined to derive the evolution of the channel bed over a length of approximately 300 m, in the main study area and upstream. The location of the channel bank tops in each cross section was marked during the field surveys. Using these markers, the banklines and channel centerline were derived. The channel bed elevation was obtained by subtracting the hydraulic radius from the average elevation of the two opposing crests of the channel banks. The hydraulic radius is defined as the cross-sectional area divided by the wetted perimeter.

3.2. Hydrological Monitoring

Discharge data were collected downstream of the study reach at a discharge station, indicated with *Q* in Figure 1c. At the discharge station, discharge is measured with an ultrasonic transit-time sensor (Flo-Sonic OCFM), which measures the transit time in two directions (upstream and downstream). The difference between these transit times is proportional the average flow velocity along the measurement path, from which the discharge is computed. The discharge estimates were acquired with a 1 h frequency. Figure 2 shows the discharge hydrograph over a period of 250 days. Water level data were measured at two locations along the study reach, indicated with WL1 and WL2 in Figure 1d. The water level gauges WL1 and WL2 started monitoring 54 and 103 days after construction of the channel had finished, respectively. Water level data were acquired with a 1 h frequency. Longitudinal water level profiles were measured using the RTK-GPS equipment during four of the five GPS surveys.

3.3. Sediment Sampling

Grain size distributions were derived from two sets of sediment samples, taken with a sediment core sampler (KC Denmark Kajak Model A). First, sediment samples were taken from the channel bed and banks just after construction had finished. Sediment samples were taken at two cross sections along the channel in the study area. Second, sediment samples were taken in the cutoff channel approximately 1 year after the construction had finished. A total of 10 cores were taken in the cutoff bend at the centerline of the constructed channel. At each location, the difference between the constructed channel and deposited sediment was determined, which ranged between 0.24 and 0.47 m below the surface. The samples were taken at two depths between the surface level and the constructed channel bed, approximately at one quarter and three quarters of the depth of the deposited sediment. Sediment samples were dried in an oven for 24 h at a temperature of 105°C. Subsequently, the sediment samples were treated with hydrogen peroxide to remove organic material. The grain size distribution was obtained using a laser particle sizer (Sympatec

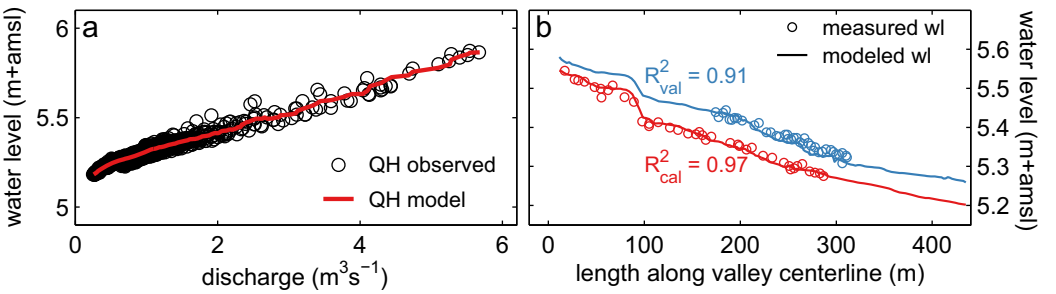

Figure 3. Input for the hydrodynamic model, with (a) discharge-water level relation (*Q-H* relation at WL2) and (b) the results of the calibration (red, $Q = 0.37$ m^3 s^{-1}) and validation (blue, $Q = 0.48$ m^3 s^{-1}) simulations, including measured and modeled longitudinal water level profiles, and the coefficient of determination R^2 as a measure of model performance.

Helos KR) and subdivided into 57 classes, ranging from 0.12 to 2000 μm. The median grain size was derived from the cumulative grain size distributions.

3.4. Hydrodynamic Model

A Reynolds Averaged Navier Stokes model (Delft3D, version 4.00.02, September 2012) [*Lesser et al*., 2004], using a k-ϵ turbulence closure, was employed to study the flow characteristics causing deposition of sediment in bend 2, prior to the chute cutoff. To minimize boundary effects in the model results in the region of interest, the model domain was extended both in lateral and longitudinal directions. For this purpose, an additional morphological survey was performed at day 133. The model domain covered an area with a length of 425 m and an average width of 39 m, indicated by the dark gray color in Figure 1d. The bathymetrical data were interpolated onto a curvilinear grid, with an average grid spacing of 2.35 m in streamwise direction and 1.25 m in cross-stream direction. A finer cross-stream grid spacing of 0.8 m in the channel section was used to account for details of the bathymetry within the channel. Ten logarithmically distributed sigma layers were defined in the vertical direction. Each sigma layer represents a constant fraction of the total depth. The logarithmically distributed sigma layers are thinner near the bed, where velocity gradients are larger. The bed shear stress vector (τ_{bx}, τ_{by}) (N m^{-2}) proceeds from the velocity gradient vector ($\partial u/\partial\sigma, \partial v/\partial\sigma$) (m s^{-1}) at the bed according to:

$$\tau_{bx} = \frac{\rho \nu_v}{h}\frac{\partial u}{\partial \sigma}\bigg|_{\sigma=-1} \tag{1}$$

$$\tau_{by} = \frac{\rho \nu_v}{h}\frac{\partial v}{\partial \sigma}\bigg|_{\sigma=-1} \tag{2}$$

where σ is the scaled vertical coordinate that takes a value of -1 at the bed, ν_v is the vertical eddy viscosity (m^2 s^{-1}) solved based on the k-ϵ turbulence closure scheme, and h is water depth (m). The horizontal eddy viscosity was set to 2.5 m^2 s^{-1}.

Discharge and water levels were imposed as upstream and downstream boundary conditions, respectively. To find the discharge conditions that could explain the deposition of sediment in bend 2, a series of steady state simulations was carried out imposing discharges ranging between 0.1 and 5.7 m^3 s^{-1}, which corresponds to the range of observed discharges in the period under study (Figure 2). In these simulations, the water level boundary condition was derived from a stage-discharge relation, based on measured water level time series at water level gauge WL2. The measured water level data from WL2 were extrapolated to the downstream boundary of the model domain, based on measured water level slopes. Figure 3a shows the *Q-H* relation and Figure 3b the longitudinal water level profile.

The model calibration was performed using the measured longitudinal water level profile from the first GPS survey. In the calibration procedure, values of the Manning's bed roughness coefficient n (m$^{-1/3}$) were varied, using calibration values of Manning's n between 0.013 and 0.027 s m$^{-1/3}$, representing sand. The 20 m long channel section consisting of peat caused an increase in water level (Figure 3b), between 80 and 100 m along the centerline coordinate. This was represented in the model by increasing the roughness in this area. For the calibration runs, values of Manning's n in the peat area were varied between 0.07 and 0.21 s m$^{-1/3}$. The optimized values of the Manning coefficients amounted to 0.017 s m$^{-1/3}$ for the sand

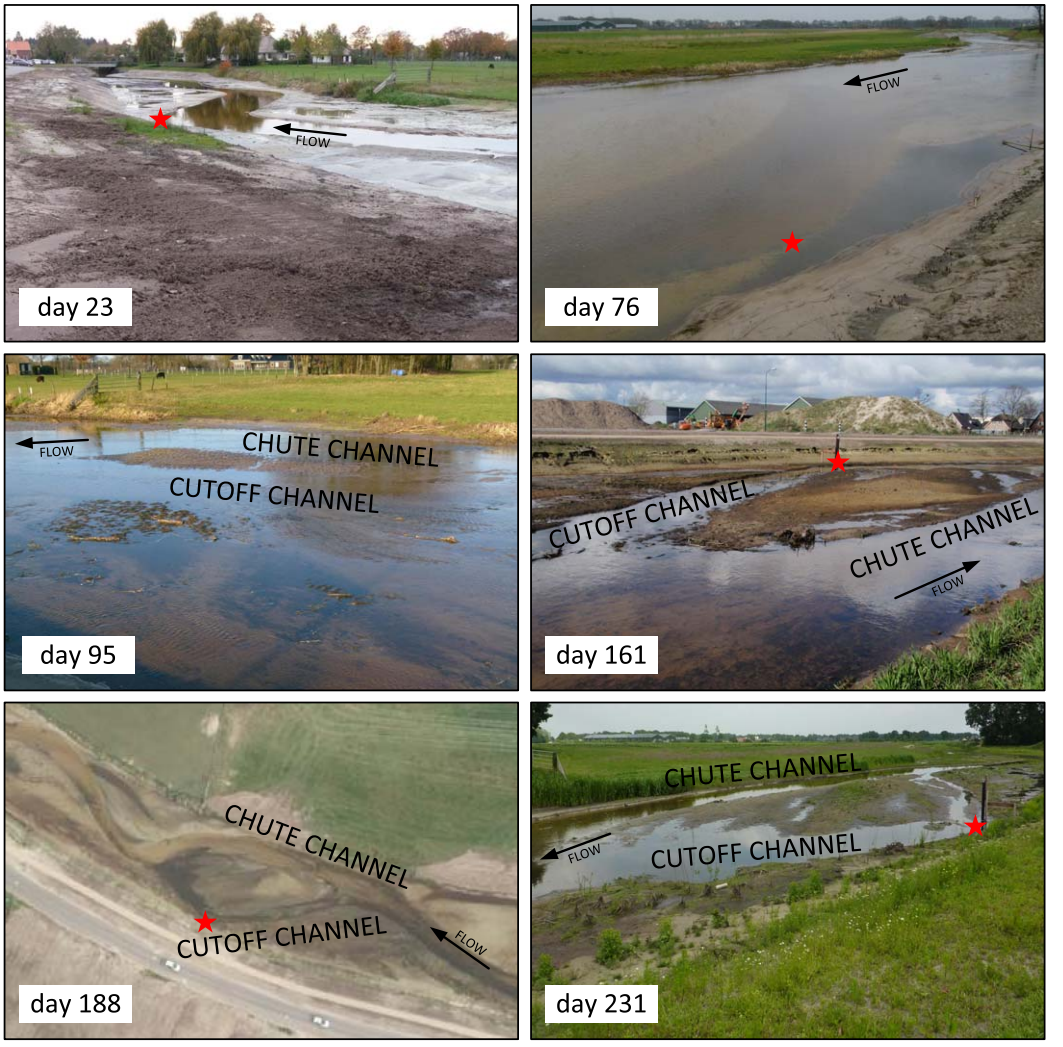

Figure 4. Sequence of photos from the study area. Photos are taken at 23, 76, 95, 161, 188, and 231 days after channel reconstruction had finished. Flow is indicated with an arrow. The red star indicates the apex of bend 3.

area and 0.14 s $m^{-1/3}$ for the peat area in the domain. This resulted in a coefficient of determination of $R^2 = 0.97$. A validation simulation was performed using the measured longitudinal water level profile from the second GPS survey. This resulted in a coefficient of determination of $R^2 = 0.91$ (Figure 3b).

4. Results

4.1. Field Results

Figure 4 shows a sequence of six photos taken between 23 and 231 days after construction of the channel. The top-left figure shows the sinuous channel planform after construction, located in a lowered floodplain. Initially, the floodplain consisted of bare soil. After 95 days, the first distinction between the constructed (cutoff) channel and chute channel became visible. In the photo taken 161 days after construction and in subsequent photos, this distinction becomes more pronounced. The aerial photo (day 188) gives a good overview of the study area after the chute cutoff occurred. Vegetation started to appear after 231 days.

Figure 5 shows on the left side the bathymetry from the six morphological surveys, and on the right side the resulting erosion and deposition in the five subsequent periods. The first survey (day 0) shows the channel was constructed according to a regular sinuous pattern, with a sinuosity $P = 1.24$. Between the first two surveys, sediment was deposited in bend 2, with sedimentation locally exceeding 0.30 m. The third survey (day 93) shows more sediment was deposited in bend 2, which had been cutoff from the main channel.

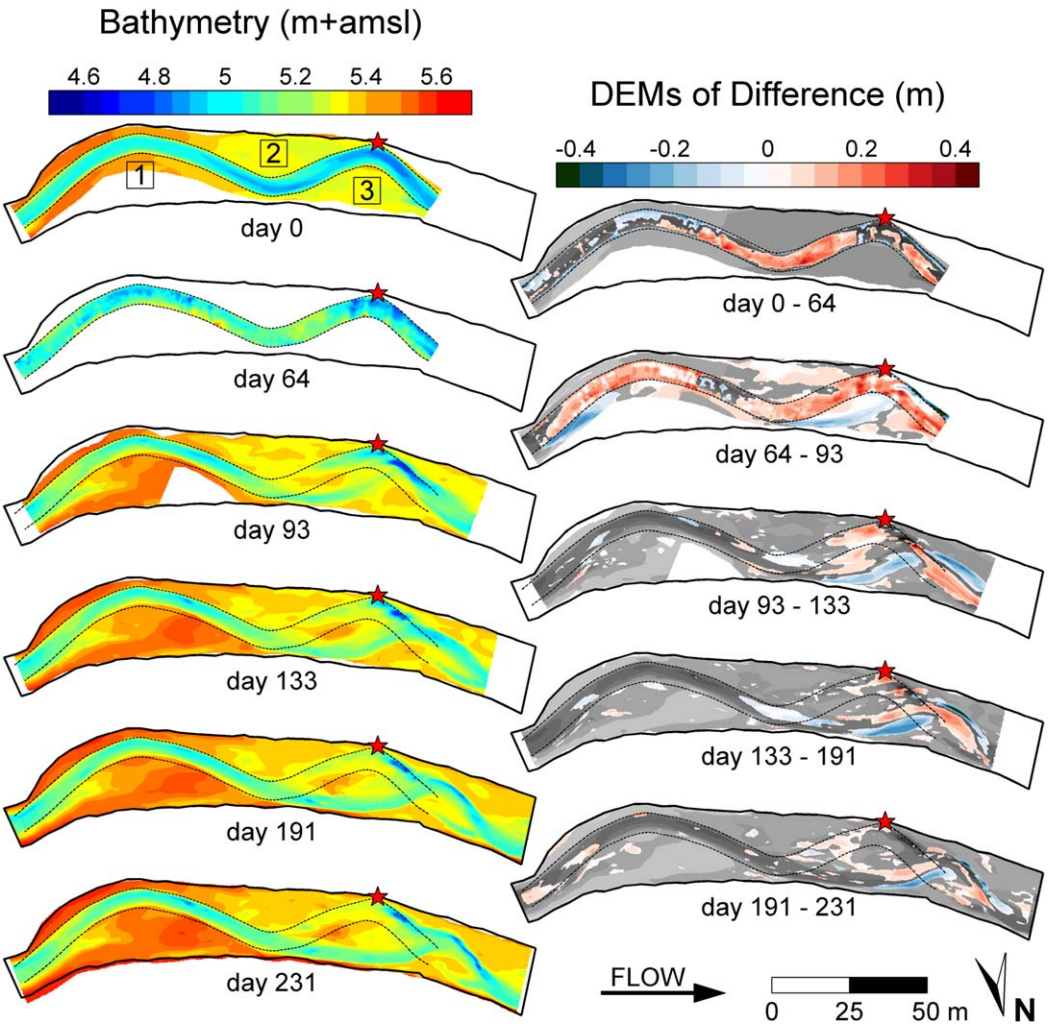

Figure 5. Digital Elevation Models and DEMs of Differences of all six morphological surveys. The number of days indicates the time since channel reconstruction had finished. The dashed black lines indicate the location of the channel banks of the constructed channel. The red star indicates the apex of bend 3, as indicated in Figure 4. On the left side of the figure, elevation is indicated in m + amsl, which denotes meters above mean sea level. On the right side of the figure, erosion is indicated in blue and deposition in red.

The process of sedimentation of the cutoff channel continued in the subsequent period, albeit only in the downstream limb of the cutoff channel. The third survey shows an embayment had formed downstream of the apex of bend 2. This embayment continued to show incision into the floodplain until the fourth survey, resulting in a clear distinction between the constructed channel (indicated with the dashed lines) and the new channel. The newly formed channel bend migrated in downstream direction between the fourth and sixth surveys, showing both erosion at the outer bank and accretion at the inner bank. Focusing on the upstream part of the study area, morphodynamic developments occurred between the second and third surveys in bend 1. In the subsequent surveys, only minor changes occurred in the upstream part of the study area.

Figure 6 shows the temporal evolution of both the channel centerline and the longitudinal bed elevation for all six morphological surveys. Morphological data obtained upstream from the main study area are also included in Figure 6b. In both figures, the *x* axis is displayed as the length along the valley centerline. Figure 6a clearly shows the cutoff occurred between the second and third surveys, after which bend 3 started to migrate in the downstream direction. When comparing the initial and final bed levels in Figure 6b, it appears that sediment was deposited in the downstream part of the study area. At the upstream end of the study area erosion occurred. This caused a dramatic reduction of the channel gradient, from 0.96 to 0.20 m km^{-1}. When looking into more detail, Figure 6b shows that bend 1 featured only minor changes throughout the survey period, with deposition of sediment between the second and third surveys being most

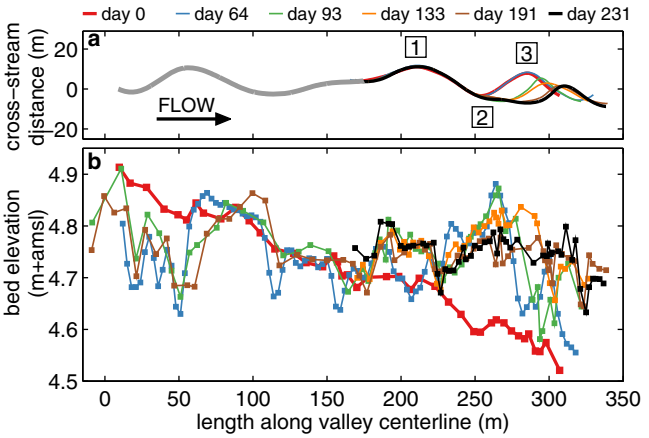

Figure 6. (a) Temporal evolution of the channel centerline, which has been derived from the morphological surveys. (b) Temporal evolution of the longitudinal bed elevation. Bed elevation is obtained at each channel cross section by averaging the measured cross-sectional data over the width of the channel bed between the channel banks.

apparent. The deposition of sediment in bend 2 had already started in the second survey, which was prior to the occurrence of the chute cutoff.

Figure 7 shows in green the grain size distribution of the sediment samples taken from the constructed channel. The figure shows in blue and red the grain size distributions of the deposited sediment in the cutoff channel, for the upper and lower half of the deposited sediment layer, respectively. The average grain size in the upper layer of the cutoff channel is finer than in the lower layer of the channel. The grain size of the constructed channel can be found in between the grain size distributions from for the upper and lower layers in the cutoff channel.

Table 2 shows the median grain size, the kurtosis and the skewness of the grain size distributions. Both the kurtosis and the skewness are lower for the samples taken in the constructed channel. Sediment deposited in the cutoff channel is thus more uniform than the sediment present in the channel directly after construction.

Figure 8 shows the sediment characteristics of the sediment samples taken in the cutoff channel. Figure 8a shows sample locations of the 10 sediment cores. Figure 8b includes the morphological evolution of the channel bed elevation in the cutoff channel and shows sediment was first deposited in the upper limb of the cutoff bend. Sedimentation gradually continued in the downstream direction, until the entire cutoff channel was filled with sediment. Figure 8c shows in more detail the distinction between the finer upper layer and the coarser lower layer. The median grain size of the upper samples is finer than the grain size of the lower samples. Besides, the plot shows a downstream fining, where the deposited sediment is coarser in the upper limb of the cutoff channel (showing an increased median grain size), both for the upper and lower samples.

4.2. Model Results

Figure 9 shows the results from the series of steady state hydrodynamic model simulations, with in Figure 9a the channel centerline from the first survey as a reference. Figure 9b shows the cross-sectional averaged bed shear stress within the channel banks, along the valley centerline. The plot also displays the critical bed shear stress:

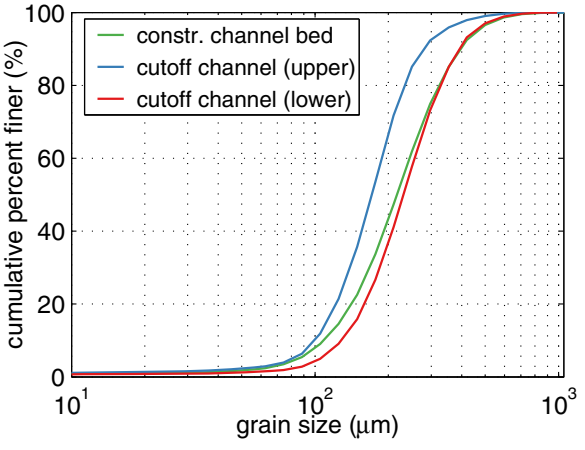

Figure 7. Grain size distributions, with the grain size distribution from the constructed channel bed in green, and the average grain size distributions of the upper and lower half of the deposited sediment in the cutoff channel in blue and red, respectively.

$$\tau_{cr} = \theta_{cr}(\rho_s - \rho)gd_{50} \quad (3)$$

where θ_{cr} is the critical Shields parameter, ρ_s is the density of sediment (kg m^{-3}), ρ is the density of water (kg m^{-3}), g is the gravitational acceleration (m s^{-2}), and d_{50} is the median grain size (m). The critical Shields parameter is defined as [*Van Rijn*, 1993]:

$$\theta_{cr} = 0.14D_*^{-0.64} \text{ for } 4 < D_* \leq 10 \quad (4)$$

where D^* is the nondimensional particle parameter:

$$D_* = \left[\frac{(s-1)g}{\nu^2}\right]^{1/3} d_{50} = 6.52 \quad (5)$$

Table 2. Statistical Parameters (Median Grain Size, Kurtosis, and Skewness) of the Sediment Samples Taken in the Constructed Channel (Day 0) and in the Cutoff Channel (Day 341)

	Median Grain Size (μm)	Kurtosis	Skewness
Constructed channel bed	218	6.9	2.3
Cutoff channel (upper)	172	10.1	2.9
Cutoff channel (lower)	234	9.3	2.7

where $s = \rho_s/\rho$ is the relative submerged specific gravity of the sediment, $g = 9.81$ m s^{-2} is the gravitational acceleration and $\nu = 10^{-6}$ m^2 s^{-1} is the kinematic viscosity of water. This results in θ_{cr}=0.042. Further attributing $\rho_s = 2650$ kg m^{-3}, $\rho = 1000$ kg m^{-3}, $d_{50} = 258$ μm, this results in the critical bed shear stress τ_{cr}=0.18 N m^{-2}.

Figure 9b shows that the bed shear stress does not exceed its critical value in the whole study area for discharges smaller than 0.4 m^3 s^{-1}. With discharges between 0.4 and 0.9 m^3 s^{-1}, τ_{cr} is exceeded in bend 1, but the shear stress remains smaller than τ_{cr} in bends 2 and 3. For discharges exceeding 0.9 m^3 s^{-1}, the bed shear stress in the entire channel exceeds τ_{cr}.

Figure 9c reveals the reason for the apparent distinction between the upstream and downstream bed shear stress regimes, showing the longitudinal water level profiles from the five steady state simulations. For the lower discharges, the water level profile is nearly linear. When discharge increases, the water level becomes bilinear, with the smallest water level slope in the downstream reach. Hence, a backwater curve appears in the upstream water level profile. This backwater curve is most likely caused by a bridge that narrows the floodplain width at the downstream end of the study reach (Figures 1d and 1e). Deceleration of the flow in the downstream part of the study area causes the flow velocities to decrease dramatically, and consequently, leads to a negative gradient in bed shear stresses.

These results imply that for a range of discharges (i.e., 0.4–0.9 m^3 s^{-1}), bed material is entrained in bend 1, since bed shear stresses exceed the critical value increasingly more in the downstream direction. Within this discharge range, bed material is likely to be deposited in bend 2, where bed shear stresses drop below

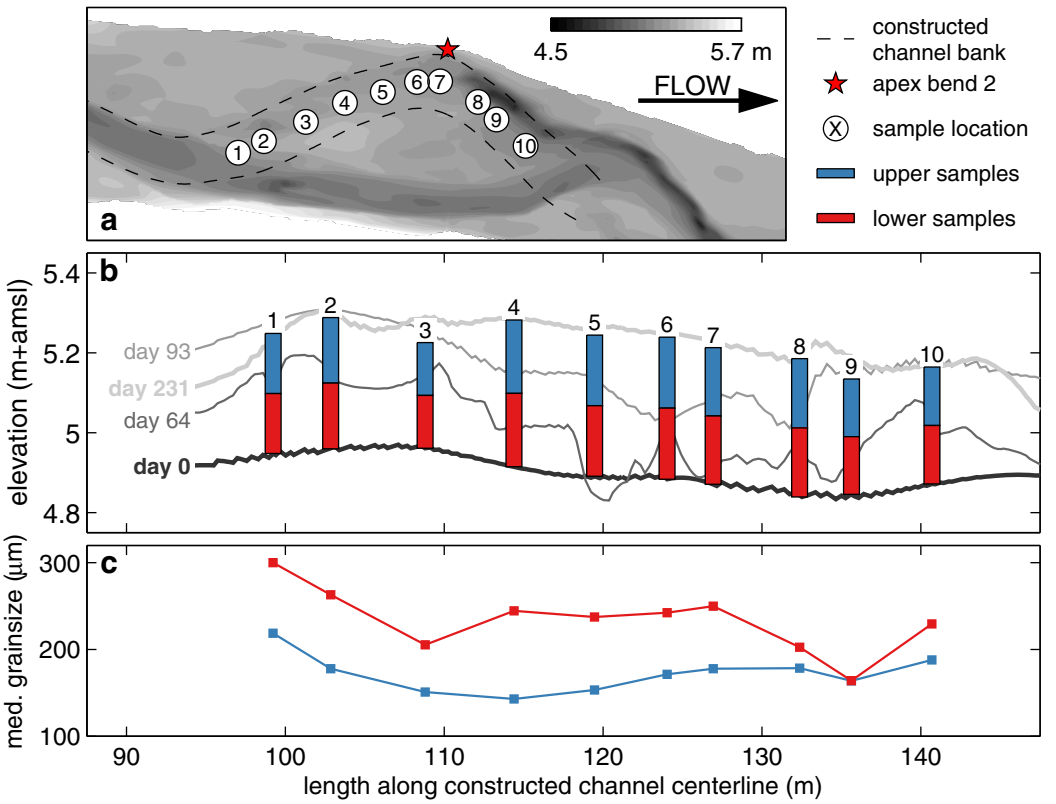

Figure 8. Results of the sediment sampling taken approximately 1 year after channel reconstruction had finished: (a) plan view of the locations of the 10 sediment cores, (b) longitudinal channel bed profile along the cutoff channel showing the locations of the upper (blue) and lower (red) sediment cores and the surface level derived from four morphological surveys, and (c) median grain sizes.

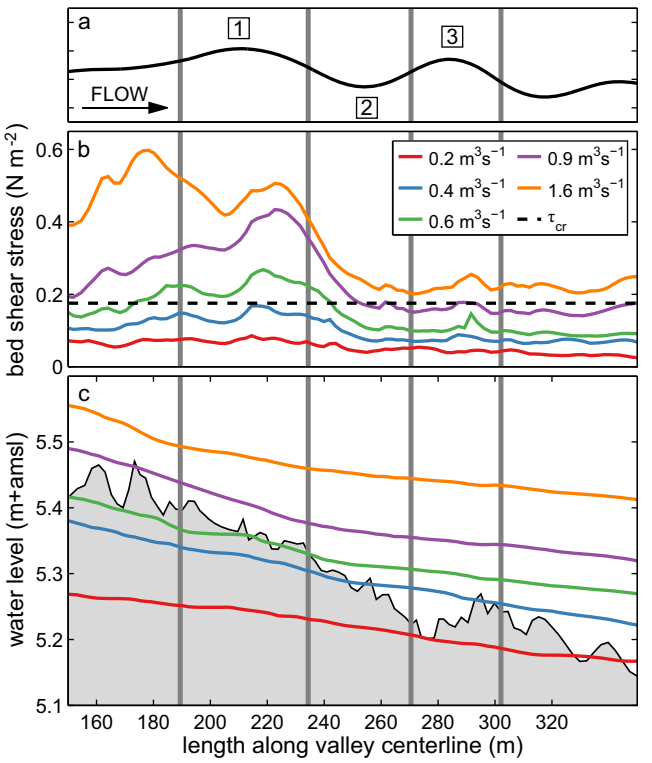

Figure 9. Results from the hydrodynamic model. (a) Constructed channel centerline. Vertical lines indicate the inflection points for the three bends. (b) Spatial distribution of the cross-sectional averaged bed shear stress for five steady state simulations, corresponding to discharges amounting to 0.2, 0.4, 0.6, 0.9, and 1.6 $m^3 s^{-1}$, respectively. The dashed line indicates the critical bed shear stress τ_{cr} (equation (3)). (c) The corresponding longitudinal water level profile, where the gray area indicates elevation below the channel banks.

the critical value and, moreover, are decreasing in downstream direction. In the period before the chute cutoff occurred, discharges remained in this discharge range for 24% of the time.

5. Discussion

5.1. Overview of Events

Figure 10 introduces a conceptual model of the main morphological processes that occurred in the period between construction and chute cutoff. Figure 10a shows the constructed channel planform (blue), within the lowered floodplain (yellow), and surrounded by pasture (green). The figure also indicates the location of the former straightened channel before channel reconstruction (brown), which was filled with sediment by the local water authority. Figure 10b presents a sketch of the deposition of sediment in bend 2 (red). This caused the flow to impinge on the point bar during flood events. An embayment formed at the apex of bend 2 (Figure 10c). The chute cutoff completed when the chute channel incised and widened into the floodplain, and more sediment was deposited in the cutoff channel. Consequently, the chute channel acted as the main channel, conveying the discharge most of the time (Figure 10d). The sequence of events can be separated into three stages. Stage 1 is the initial period leading to cutoff vulnerability, stage 2 is the cutoff, and stage 3 is adjustment to the cutoff. Hereafter, we discuss the causes and effects for each stage separately.

5.2. Stage 1: Initial Period Leading to Cutoff Vulnerability

Considering the chute cutoff as a specific form of avulsion, *Schumm* [2005] presents four groups of causes, each described in terms of the ratio S_a/S_e. Herein, S_a is the slope of the potential avulsion course and S_e is the gradient of the existing channel. Changes in S_a/S_e in the period between reconstruction and the chute cutoff are negligible, which places the event in the group for which possible causes include changes in flood peak discharge, increased sediment load, vegetative encroachment, log jams, and ice jams. Vegetation encroachment nor logs and ice played a role, which points to flood peak discharge and increased sediment load as the main causes. When viewing the stream before and after the reconstruction as a single entity, the sinuosity increase is regarded as the main cause of avulsion. Alternatively, river restoration can be seen as a separate group when categorizing causes of avulsion. This group may not only accommodate channel realignment, but also river training works such as cross vanes [*Endreny and Soulman*, 2011].

The bar deposited in the upstream limb of the cutoff bend can be interpreted as a plug bar [*Fisk*, 1944]. Natural plug bars in cutoff channels typically form in postcutoff periods [e.g., *Johnson and Paynter*, 1967; *Hooke*, 1995], when peak discharges formative for the chute channel have receded, and moderate discharges are divided over the parallel channels. Subsequently, flow is mainly concentrated in the steeper chute channel, causing channel incision and widening into the floodplain. In the cutoff channel subject to study, however, flow velocities drop below the critical value, causing deposition of sediment in the form of a plug bar. This plug bar can be considered the cause of the chute cutoff event, rather than a consequence. The

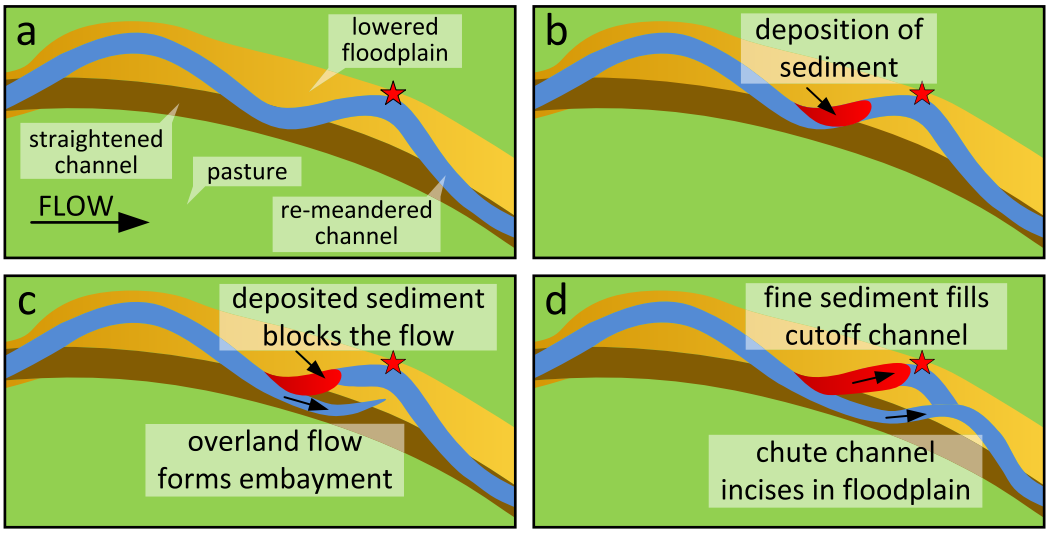

Figure 10. Conceptual model of the main morphological processes showing three stages in the development of the chute cutoff: (a) constructed remeandered channel within the lowered floodplain and the location of the former straightened channel, (b) stage 1: the initial period leading to cutoff vulnerability, (c) stage 2: the cutoff, and (d) stage 3: adjustment to the cutoff.

observations confirm two recent laboratory experiments, reporting on precutoff plug bar formation [*Peakall et al.*, 2007; *Van Dijk et al.*, 2012]. In the experiments by *Van Dijk et al.* [2012], plug bars formed in response to an increase of overbank flow, causing deceleration of flow velocity, similar to the field observations reported here.

5.3. Stage 2: Cutoff

The observations suggest a relatively large discharge eventually triggered the cutoff occurrence. Similarly, large river avulsions can be triggered by a flood event [*Slingerland and Smith*, 2003]. In natural chute cutoffs [*Constantine et al.*, 2010], the new channel is commonly located at the outer banks of meander bends, where flow velocities are high, confining levees are narrow, and flood flows impinge the banks at high angles [*Slingerland and Smith*, 2003]. Depending on the proximity to the threshold of cutoff, a flood event may not be a prerequisite. Alternative theories for triggering of the event can be considered, including seepage flow, headcut propagation, and swale enlargement. Seepage flow can weaken the strength of a bank against erosion and is a known cause for neck cutoff [*Han and Endreny*, 2014] and initiation of meandering [*Eekhout et al.*, 2013]. There were no signs of seepage, and the elevation differences may be too small for a significant seepage flow to be generated. Swale enlargement and headcut propagation are also unlikely to be relevant, since neither a headcut nor a clear swale in the floodplain area were observed where the cutoff channel developed.

Figure 10c shows the initial chute channel formation coincides with a location where the former channel used to be located. The former channel was filled with sediment prior to the construction of the new channel. It is very likely that the sediment fills in the former channel were less consolidated than the rest of the floodplain. Less consolidated material may lead to preferential hyporheic flows across the old channel path, leading to sediment loss, and pore enlargement. Therefore, the corresponding floodplain area was prone to erosion. The aerial photo in Figure 11 clarifies this observation. The photo shows that at several other locations, especially upstream from the main study area, erosion occurred in the floodplain where the former straightened channel used to be. The case study presented here illustrates that water authorities need to take into consideration the high erodibility of former channels filled with sediment.

5.4. Stage 3: Adjustment to the Cutoff

Despite the artificial setting under which the cutoff event occurred, the postcutoff morphodynamics bear similarities with existing studies in more natural settings [*Hooke*, 1995; *Fuller et al.*, 2003; *Zinger et al.*, 2013]. These describe the sequence of morphological developments in the chute channel following the cutoff, showing bed scour followed by a period characterized by extensive bank erosion and lateral channel

Figure 11. Aerial photo taken at day 188 after channel reconstruction had finished. The shaded area shows the location of the former straightened channel before the construction of the new channel. Erosion is observed where the former straightened channel used to be, at four locations along the reconstructed channel, indicated with the red ovals.

migration [*Hooke*, 1995; *Fuller et al*., 2003] and channel widening [*Zinger et al*., 2013]. After the initial chute channel had formed in the case study presented here, the channel gradually incised and widened into the floodplain, and the channel bend migrated in the downstream direction, consistent with previous observations [*Hooke*, 1995; *Fuller et al*., 2003]. These observations show a morphological response driven by sharp curvature of the flow adjusting to the geometry downstream of the chute channel.

In a future effort, the obtained data set presented here can serve to improve the predictive capacity of morphodynamic models aiming to simulate channel adjustments in response to a variable discharge. The detailed observations of the systematic channel migration in response to formation of the chute channel can be used to study the physical mechanism responsible for the link between bank erosion and bank accretion on opposite sides of the downstream section of the channel. A calibrated and validated morphological model would allow to investigate why the observations do not show signs of local scour, headcut, or a clear zone of deposition in the region downstream of the cutoff channel.

5.5. Possible Role of Backwater in Natural Chute Cutoffs

Discharge variation and backwater effects are omnipresent in lowland rivers connected to lakes and floodplain ponds [e.g., *Hidayat et al*., 2011]. The observations in the Lunterse Beek lead to the hypothesis that backwater can form a plug bar and trigger a chute cutoff event in such rivers because the cause of backwater is irrelevant to the mechanism leading to chute cutoff. Backwater lengths in deltas were recently found to correspond with the river location where avulsion has taken place [*Chatanantavet et al*., 2012]. The location of bends where chute cutoff events have occurred may be related to the backwater lengths associated with a river-connected lake.

6. Conclusions

In a restored lowland stream, subject to a relatively natural, flashy discharge, a chute cutoff occurred within 3 months after construction of a stream restoration project. As part of a research project to establish postproject morphological changes in this stream restoration project, a detailed monitoring plan was implemented. This allowed an unprecedented opportunity to analyze the bathymetry before, during and after a chute cutoff event. Despite the relatively artificial setting, the event bears similarities with natural cutoffs. The field results agree with the following inferences from previous, more indirect studies: (1) sediment was deposited in the upstream limb of the cutoff channel, prior to the cutoff event, (2) an embayment formed along the outer bank, upstream of the meander that underwent cutoff, (3) the chute channel incised and widened into the floodplain, and (4) the deposited sediment in the cutoff channel showed upward fining. The detailed description presented herein points to an important role of backwater effects in triggering the sequence of events, by forming a plug bar. The embayment following the plug bar initiated at a location where the former channel was located, i.e. where the erosion resistance may expected to be low. An aerial photograph reveals morphological activity in the lowered floodplain where the former channel was located, whereas on other locations no morphological changes were observed. The main morphological process that led to the chute cutoff, i.e. agradation of the channel bed, shows similarities with processes of channel avulsion, which occur in net-depositional river systems. The data set presented here, including the morphological evolution before and during the chute cutoff, may serve to improve morphodynamic models aiming to simulate channel adjustments in river systems with a variable discharge.

Acknowledgments
This study is part of a research project funded by the STOWA, the Foundation for Applied Water Research (project 443209) and the research project Beekdalbreed Hermeanderen funded by Agency NL (project KRW 09023). The obtained field data are freely available at http://dx.doi.org/10.6084/m9.figshare.960038. We thank water board Vallei en Veluwe for the support in data collection. We thank Philip Wenting (Wageningen University) for his contribution to the fieldwork campaign, and Bart Vermeulen and Paul Torfs (Wageningen University) for their help in postprocessing of field data. We thank Roy Laseroms (LWRO) and Waterschap Vallei en Veluwe for providing the data from the ADCP survey and CycloMedia Technology B.V. for providing the aerial photo. We thank Remko Uijlenhoet (Wageningen University) and Piet Verdonschot (Alterra) for their comments on this paper.

References

Braudrick, C. A., W. E. Dietrich, G. T. Leverich, and L. S. Sklar (2009), Experimental evidence for the conditions necessary to sustain meandering in coarse-bedded rivers, *Proc. Natl. Acad. Sci. U. S. A.*, *106*, 16,936–16,941.

Brush, L. M., and M. G. Wolman (1960), Knickpoint behaviour in noncohesive material: A laboratory study, *Geol. Soc. Am. Bull.*, *71*, 59–73.

Chatanantavet, P., M. P. Lamb, and J. A. Nittrouer (2012), Backwater controls of avulsion location on deltas, *Geophys. Res. Lett.*, *39*, L01402, doi:10.1029/2011GL050197.

Constantine, J. A., S. R. Mclean, and T. Dunne (2010), A mechanism of chute cutoff along large meandering rivers with uniform floodplain topography, *Geol. Soc. Am. Bull.*, *122*, 855–869.

Dieras, P. L., J. A. Constantine, T. C. Hales, H. Piégay, and J. Riquier (2013), The role of oxbow lakes in the off-channel storage of bed material along the Ain River, France, *Geomorphology*, *188*, 110–119.

Dufour, S., and H. Piégay (2009), From the myth of a lost paradise to targeted river restoration: Forget natural references and focus on human benefits, *River Res. Appl.*, *25*, 568–581.

Eekhout, J. P. C., A. J. F. Hoitink, and B. Makaske (2013), Historical analysis indicates seepage control on initiation of meandering, *Earth Surf. Processes Landforms*, *38*, 888–897.

Eekhout, J. P. C., R. G. A. Fraaije, and A. J. F. Hoitink (2014a), Morphodynamic regime change in a reconstructed lowland stream, *Earth Surf. Dyn.*, *2*, 279–293.

Eekhout, J. P. C., A. J. F. Hoitink, J. H. F. de Brouwer, and P. F. M. Verdonschot (2014b), Morphological assessment of reconstructed lowland streams in the Netherlands, *Adv. Water Resour.*, doi:10.1016/j.advwatres.2014.10.008.

Endreny, T., and M. Soulman (2011), Hydraulic analysis of river training cross-vanes as part of post-restoration monitoring, *Hydrol. Earth Syst. Sci.*, *15*, 2119–2126.

Erskine, W., C. McFadden, and P. Bishop (1992), Alluvial cutoffs as indicators of former channel conditions, *Earth Surf. Processes Landforms*, *17*, 23–37, Miss. River Comm., Vicksburg, Miss.

Fisk, H. N. (1944), Geological Investigation of the Alluvial Valley of the Lower Mississippi River, 78 pp., U.S. Dep. of the Army, Miss. River Comm.

Fuller, I. C., A. R. G. Large, and D. J. Milan (2003), Quantifying channel development and sediment transfer following chute cutoff in a wandering gravel-bed river, *Geomorphology*, *54*, 307–323.

Gay, G. R., H. H. Gay, W. H. Gay, H. A. Martinson, R. H. Meade, and J. A. Moody (1998), Evolution of cutoffs across meander necks in Powder River, Montana, USA, *Earth Surf. Processes Landforms*, *23*, 651–662.

Ghinassi, M. (2011), Chute channels in the Holocene high-sinuosity river deposits of the Firenze plain, Tuscany, Italy, *Sedimentology*, *58*, 618–642.

Grenfell, M., R. Aalto, and A. Nicholas (2012), Chute channel dynamics in large, sand-bed meandering rivers, *Earth Surf. Processes Landforms*, *37*, 315–331.

Han, B., and T. A. Endreny (2014), Detailed river stage mapping and head gradient analysis during meander cutoff in a laboratory river, *Water Resour. Res.*, *50*, 1689–1703, doi:10.1002/2013WR013580.

Hickin, E. J., and G. C. Nanson (1975), The character of channel migration on the Beatton River, north-east British Columbia, Canada, *Geol. Soc. Am. Bull.*, *86*, 487–494.

Hidayat, H., B. Vermeulen, M. G. Sassi, P. J. J. F. Torfs, and A. J. F. Hoitink (2011), Discharge estimation in a backwater affected meandering river, *Hydrol. Earth Syst. Sci.*, *15*, 2717–2728.

Hooke, J. M. (1995), River channel adjustment to meander cutoffs on the River Bollin and River Dane, northwest England, *Geomorphology*, *14*, 235–253.

Howard, A. D. (1996), Modelling channel evolution and floodplain morphology, in *Floodplain Processes*, edited by P. A. Carling, and G. E. Petts, pp. 15–62, John Wiley & Sons, Chichester, U. K.

Jin, D., and S. A. Schumm (1987), A new technique for modeling river morphology, in *International Geomorphology, Part I*, edited by V. Gardiner, pp. 681–690, John Wiley, Chichester, U. K.

Johnson, R. H., and J. Paynter (1967), Development of a cutoff on the River Irk at Chadderton, Lancashire, *Geography*, *52*, 41–49.

KNMI (2014), Langjarige gemiddelden en extremen, tijdvak 1971–2000, De Bilt, Netherlands. [Available at http://www.knmi.nl/klimatologie/normalen1971–2000/index.html.]

Langendoen, E. J. (2011), Application of the CONCEPTS channel evolution model in stream restoration strategies, in *Stream Restoration in Dynamic Fluvial Systems*, edited by A. Simon, S. J. Bennett, and J. M. Castro, pp. 487–502, American Geophysical Union, Washington, D. C.

Lesser, G. R., J. A. Roelvink, J. A. T. M. van Kester, and G. S. Stelling (2004), Development and validation of a three-dimensional morphological model, *Coastal Eng.*, *51*, 883–915.

McGowen, J. H., and L. E. Garner (1970), Physiographic features and stratification types of coarse-grained point bars: Modern and ancient examples, *Sedimentology*, *14*, 77–111.

Micheli, E. R., and E. W. Larsen (2011), River channel cutoff dynamics, Sacramento River, California, USA, *River Res. Appl.*, *27*, 328–344.

Milan, D. J., G. L. Heritage, A. R. G. Large, and I. C. Fuller (2011), Filtering spatial error from DEMs: Implications for morphological change estimation, *Geomorphology*, *125*, 160–171.

Peakall, J., P. J. Ashworth, and J. L. Best (2007), Meander-bend evolution, alluvial architecture, and the role of cohesion in sinuous river channels: A flume study, *J. Sediment. Res.*, *77*, 197–212.

Schumm, S. A. (2005), *River Variability and Complexity*, Cambridge Univ. Press, Cambridge, U. K.

Slingerland, R., and N. D. Smith (2003), River avulsions and their deposits, *Annu. Rev. Earth Planet. Sci.*, *32*, 257–285.

Thompson, A. (1984), Long and short-term channel change in gravel-bed rivers, PhD thesis, 543 pp., Univ. of Liverpool, Liverpool, U. K.

Van Dijk, W. M., W. I. Van de Lageweg, and M. G. Kleinhans (2012), Experimental meandering river with chute cutoffs, *J. Geophys. Res.*, *117*, F03023, doi:10.1029/2011JF002314.

Van Dijk, W. M., F. Schuurman, W. I. van de Lageweg, and M. G. Kleinhans (2014), Bifurcation instability and chute cutoff development in meandering gravel-bed rivers, *Geomorphology*, *213*, 277–291.

Van Rijn, L. C. (1993), *Principles of Sediment Transport in Rivers, Estuaries and Coastal Seas*, 700 pp., Aqua Publ., Blokzijl, Netherlands.

Zinger, J. A., B. L. Rhoads, and J. L. Best (2011), Extreme sediment pulses generated by bend cutoffs along a large meandering river, *Nat. Geosci.*, *4*, 675–678.

Zinger, J. A., B. L. Rhoads, J. L. Best, and K. K. Johnson (2013), Flow structure and channel morphodynamics of meander bend chute cutoffs: A case study of the Wabash River, USA, *J. Geophys. Res. Earth Surf.*, *118*, 2468–2487, doi:10.1002/jgrf.20155.